Advanced Materials, *23*, 5275–5282 **(2011)**

Immobilized biocatalysts: novel approaches and tools for binding enzymes to supports

P. Torres-Salas[a], A. del Monte-Martinez[b], B. Cutiño-Avila[b], B. Rodriguez-Colinas[a], M. Alcalde[a], A.O. Ballesteros[a] and F.J. Plou[a,*].

[a] *Departamento de Biocatálisis, Instituto de Catálisis y Petroleoquimica, CSIC, Cantoblanco, 28049 Madrid, Spain.*

[b] *Centro de Estudio de Proteínas, Facultad de Biología, Universidad de La Habana, MES, 10400 Ciudad de La Habana, Cuba.*

*Corresponding author: Francisco J. Plou, Departamento de Biocatálisis, Instituto de Catálisis y Petroleoquímica, CSIC, Marie Curie 2, 28049 Madrid, Spain. Phone: 34-91-5854869. Fax: 34-91-5854760; E-mail: fplou@icp.csic.es.

ABSTRACT

In the last decade, new trends for enzyme attachment to solid carriers have emerged in an attempt to rationalize the classical methods for enzyme immobilization. *In silico* analysis is becoming a powerful tool to predict the orientation of the enzyme covalently-attached to the carrier or the protein regions involved in the adsorption to the support. Significantly, an array of algorithms has been established for the Rational Design of Immobilized Derivatives (RDID), which comprises both the protein size and the textural properties of the support. Ordered mesoporous materials open a challenging pathway to tailor immobilized enzymes with high volumetric activity and minimum lixiviation. In addition, fluorescence confocal microscopy is being successfully employed to understand the diffusional restrictions and the distribution of biomolecules within the support.

Keywords: Enzymes, Covalent immobilization; Rational Design of Immobilized Derivatives (RDID); Ordered mesoporous materials; Fluorescence confocal microscopy; In silico analysis

1. Introduction

The new advances in chemical catalysis and biocatalysis are determinant in reducing the environmental footprint of chemical processes and petroleum-based technologies. In particular, biocatalysis fully participates in the "*green chemistry*" concept that was introduced in the 90s and whose impact on sustainability is now established beyond any doubt.[1] In the new post-genomic era, the marriage between system and synthetic biology guarantees the success of the enzyme engineering for practical uses. However, the design of effective immobilization methods represents one of the main hurdles that hamper to set up industrial-scale biocatalytic processes.[2,3] Essentially, enzyme immobilization allows easy separation and reuse of the biocatalyst, makes the product recovery easier and very often enhances enzyme resistance against inactivation by different denaturant agents (including extreme pHs or high temperatures, the presence of organic co-solvents, inhibitors and more). Apart from their application as reusable heterogeneous biocatalysts, immobilized enzymes are proper platforms on which developing stable nanobiodevices for analytical, energetic and biomedical applications (*e.g.* biosensors, biofuel cells), as well as tools for solid-phase protein chemistry or microdevices for controlled release of protein drugs.[4]

The enzyme immobilization protocols described in literature can be sorted into three main groups: (1) enzyme binding to a prefabricated support, (2) enzyme entrapment or encapsulation, where a polymeric 3D-network is formed in the presence of the enzyme, and (3) carrier-free cross-linking with bi-functional reagents (*i.e.* cross-linked enzyme crystals –CLECS- and aggregates –CLEAS–).[2]

When designing a reliable immobilization method, the non-catalytic requirements (separation, reuse, downstream processing, etc.) as well as the catalytic functions (productivity, space-time yield, productivity, etc.) must be taken into

account.[5] In most of the cases, the immobilization protocols are roughly developed on empirical basis,[5] and are based on the observation that a certain carrier has proven its efficiency with a broad number of enzymes.[6] For that reason, the design of robust immobilized biocatalysts can be considered "irrational" because it results from screening of several methodologies; in consequence, many industrial processes might be operating under suboptimum conditions. In this scenario, the new *in silico* analysis provide a fresh twist in enzyme immobilization. Indeed, this approach helps to immobilize enzymes *ad-hoc*, by predicting the location of amino acid residues or protein domains implicated in the binding with the support. The combination of *in silico* analysis by molecular modelling with experimental research is widely used in biocatalysis,[7] but only of recent application in enzyme immobilization. Hudson *et al.* were pioneers in conducting *in silico* studies before experimental work for the immobilization of two enzymes (cytochrome c and xylanase) in mesoporous materials.[8] After analyzing the physicochemical properties of several mesoporous silica (including isoelectric points and zeta potentials) as well as the surface potential of the biomolecules, they were able to predict the best combinations protein-carrier that maximize the polar, ionic and/or hydrophobic interactions. Very recently, Weber *et al*. studied the adsorption of P450 enzymes on mesoporous MCM-41 and SBA-15;[9] modelling the 3D enzyme structure and performing electrostatic potential calculations, they predicted the pH-dependence of the P450 immobilization and proposed the possible orientations of the protein on such mesoporous materials.

On the other hand, the selection of a proper support is essential in this field. Currently, a broad collection of new carriers for enzyme immobilization are coming up, allowing the researchers to specifically choose "*a la carte*" different features depending on the enzyme and the given application (*e.g.* particle size, chemical functionality,

length of spacer arm, porosity, the hydrophile-lipophile balance of the microenvironment surrounding the enzyme, and more).[10-12] Table 1 summarizes the different types of materials that have been investigated as enzyme carriers, including the strategies developed for enzyme immobilization. The mechanical strength, the chemical and physical stability of the carrier, the maximum enzyme loading, the leakage or the final manufacturing costs are other properties to be considered for the implementation of the enzyme immobilized system into an specific industrial setting.

2. Computational methods applied to covalent binding of enzymes to supports

Binding of enzymes to supports can be generally achieved by physical means (adsorption) or chemical modification (covalent bonds). Covalent immobilization has the main advantage of forming strong and stable linkages between the enzyme and the carrier, which prevents the loss of activity caused by enzyme leakage from the support, giving rise to a robust biocatalyst.[32] Inorganic and organic materials -*e.g.* porous silica, alumina, acrylic resins or agarose (Sepharose)- can be chemically activated by different strategies with the ultimate goal of covalently attaching enzymes.[33] However, the number of commercial activated carriers for covalent immobilization is relatively small compared with available enzyme adsorbent materials.

The covalent binding of enzymes to solid supports can effectively prolong the lifetime of the biocatalysts by protecting the protein three-dimensional (3D) structure and may result in enhanced enzyme activity and stability as compared with that of the native counterpart. There are numerous protocols to covalently immobilize proteins involving different amino acid side chains of the enzyme and various activating groups in the supports;[34-37] some of them are depicted in **Figure 1**.

Supports activated with epoxy (oxirane) groups seem to be almost ideal systems for enzyme immobilization since epoxy groups are very stable at neutral pH even in wet conditions, and may be utilized to immobilize enzymes through multipoint covalent attachment with their amino (**Figure 1, a1**), phenolic (**Figure 1, a2**) and thiol groups at alkaline pH, or with carboxylic acids at moderately acid pH.[21,38] Eupergit C,[39] Sepabeads EC-EP,[21] and Dilbeads[22] are epoxy-activated carriers with high reactive groups density. However, epoxy-supports show low immobilization recoveries with highly glycosylated enzymes because the polysaccharide fraction shields the active groups in the protein surface. Amino-functionalized polymers can be used as immobilization carriers by glutaraldehyde activation followed by reaction with amino groups on the enzyme surface (**Figure 1, b1**) or with the carbohydrate moieties in glycosylated enzymes by formation of cyclic acetals (**Figure 1, b2**). The lower hydrophobicity of the amino-activated support gives rise to a better solvation by water, which in turn renders a higher immobilization recovery compared to the epoxy polymer.[6] Hetero-functional amino-epoxy supports have been also developed in order to combine the hydrophilic properties of amino supports with the reactivity of oxirane groups resulting in a faster immobilization process even at low ionic strength.[35] Activation of natural or synthetic polymers with cyanogen bromide is another enzyme immobilization method implicating the amino groups (**Figure 1c**), although the isourea bond formed is moderately stable.[40] Reversibly soluble polymers bearing carboxyl groups such as Eudragit enable efficient immobilization via the carbodiimide-mediated coupling with enzyme amino groups.[41] The physical state of such polymers can be simply controlled by a simple change of pH. It is noteworthy that the formation of covalent bonds between the enzyme and the support is favoured by the fact that the

reaction takes place on a solid phase; therefore, the synthesis/hydrolysis equilibrium is shifted towards the bond formation.[42]

In general, the reactivity of the amino acid residues of the enzyme depends on factors such as their intrinsic chemical nature, the microenvironment and, in particular, their state of ionization (controlled by the pH). It is highly desirable to establish the priority of reactivity of the different amino acid residues of the protein to predict the possible conformation of the enzyme in the immobilized derivative. In this context, the *LIGRe* algorithm (*Ligand Interacting Group Reactivity*) was recently defined for a particular amino acid;[24] it represents the proportion between active (*e.g.* deprotonated in the case of NH_2) and inactive (*e.g.* protonated) groups at immobilization pH according to Equation 1:

$$\boldsymbol{LIGRe = 10^{(pH - pK_a)}} \qquad (1)$$

The theoretical basis for this calculation resides on the classical Henderson-Hasselbalch equation. When *LIGRe* < 0.1 the reactivity of the ionizable group can be considered low; if 0.1 < *LIGRe* < 1 the residue can be considered half-reactive, and if *LIGRe* ≥ 1 it is considered reactive.[43]

Using this algorithm, we have analyzed the reactivity of amino and phenolic residues of the *Myceliophthora thermophila* laccase (MtL) on the solvent accessible area during its covalent immobilization on a polymethacrylate-based polymer (Sepabeads® EC-EP3) activated with epoxy groups (unpublished material). Laccases are multi-copper containing oxidases (EC 1.10.3.2) that catalyze the oxidation of phenolic compounds, with the concomitant reduction of oxygen to water, and find applications in bioremediation, paper pulp bleaching, finishing of textiles or bio-fuel cells.[44] The corresponding pK_a values of MtL residues were estimated from the PROPKA web interface.[45] **Table 2** summarizes the *LIGRe* results for laccase interacting groups at pH

9.0. Thiol residues (cysteines) are also able to react with the epoxy moieties of the polymer; however, they were excluded from the analyses because one of them was buried and the remaining six were forming disulfide bridges. At pH 9.0, the NH_2-terminal (N-Term) can be considered fully reactive. Only two lysine residues and three tyrosines presented half-reactivity at pH 9.0 (**Table 2**). It is remarkable that many covalent immobilization protocols on epoxy-activated supports are performed at pH 8.0 or even lower, which in terms of the ionization state of the reacting groups is far away of the optimum pH value, as the reactivity is about 10-fold lower than at pH 9.0.

Computational simulations offer the possibility to visualize the regions of enzymes prone to establish covalent bonds with supports.[6] We determined the most probable MtL conformation when it was immobilized at pH 9.0 and if such conformation was catalytically competent. At pH 9.0 the highest likelihood of reaction with support epoxy groups corresponded to the NH_2-terminal (N-Term). This covalent bond would give rise to an optimal conformation, as the N-Term was almost opposite to the active site of the enzyme (**Figure 2a-d**) (the immobilized biocatalyst is displaced 10˚ from the vertical, forming an angle of 80˚ with the support surface). Two other ε-NH_2 (Lys128 and Lys339), with a reactivity two orders of magnitude lower than the N-Term (**Table 2**), appear on the protein accessible surface area and were located far away from the active site, thus yielding competent conformations as well. At pH 10.0 the increase on reactivity of other ε-NH_2 on the protein solvent accessible area (Lys205, Lys325 and Lys454) could affect the catalytic efficiency of the immobilized derivative as they were in close proximity to the active site (**Figure 2e**). Concerning tyrosine residues, the analysis at pH 9.0 indicated that Tyr286 and Tyr391, with a reactivity at least 10-fold lower than N-Term (**Table 2**), offered an optimal orientation for the immobilized derivative. However, another phenolic side-chain with half reactivity

(Tyr214) was located in the vicinity of the active site (**Figure 2e**), and could exert a negative effect on the catalytic efficiency of the immobilized derivative if it eventually participates in the covalent binding. The reactivity of other tyrosines placed at the surrounding of the active-site (esp. Tyr305) seemed to be increased substantially at pH 10.0. In conclusion, *LIGRe* prediction leads to select pH 9.0 as the optimal immobilization pH in terms of protein orientation with acceptable group reactivity.

3. *In silico* analysis of adsorption of enzymes to supports

Adsorption is the simplest and oldest method for immobilizing an enzyme onto a water-insoluble support. Adsorption of enzymes onto carriers can involve physical adsorption (via non-specific forces such as hydrogen bonds or van der Waals forces), ionic binding (based on the charge-charge interaction between the carrier and the enzymes) or hydrophobic interactions between non-polar regions of the enzyme and carrier. Adsorbed biocatalysts are easily desorbed by changes in substrate and salt concentrations, or even by temperature fluctuations.[46,47] In addition, interactions with supports can cause partial deactivation of the enzyme, thereby reducing its catalytic activity. Despite the abovementioned drawbacks, adsorbed enzymes are widely employed in different industries, especially in non-aqueous media, where the enzyme lixiviation is notably minimized.[47-49]

The amount of adsorbed enzyme depends on the size of the protein molecule, the specific surface area of the carrier, the pore size and volume, and the number of sites available for protein adsorption. Recently, the Rational Design of Immobilized Derivatives (RDID), implemented into the $RDID_{1.0}$ software, has been proposed for optimization of immobilization processes.[43] Thus, an algorithm was defined to calculate the theoretical maximum amount of enzyme that can be adsorbed on a

particular support (*tMQ*, *theoretical maximum protein quantity*), also applicable to covalent immobilization. In short, assuming that the protein projection on the support surface could be considered as a circle, the maximum number of protein molecules adsorbed on a monolayer (*total support covering particles*, *TSCP*) can be calculated as:

$$TSCP = \frac{S_{BET}}{\pi (MD/2)^2} \qquad (2)$$

Here S_{BET} is the specific surface area of the support and *MD* is the average protein diameter. *TSCP* can be divided by the Avogadro's number (N_A) in order to obtain the molar maximum protein quantity (*mMQ*):

$$mMQ = \frac{TSCP}{N_A} \qquad (3)$$

Finally, *tMQ* (commonly expressed in mg of protein per gram of support) can be calculated as shown in equation 4, in which *MM* is the protein molecular mass:

$$tMQ = mMQ \times MM \qquad (4)$$

Table 3 shows RDID predictions for the *M. thermophila* laccase immobilization in various carriers (unpublished results). Polypropylene (Accurel EP-100) and the anion-exchange resin Amberlite IRA-900 showed the highest *tMQ* values (261 and 793 mg per gram of support, respectively) However, the calculation of *tMQ* assumes ideal conditions and the possible diffusional restrictions are not considered. In fact, BET surface area is measured following the adsorption of a small molecule (N_2). A generally accepted principle is that, for unrestricted access to occur, the diameter of entry pores must be at least 4 to 5 times higher than the size of the enzyme molecule.[50] New algorithms that consider the relationship between support pore size and the protein diameter have been proposed and implemented in the $RDID_{1.0}$ software (data not shown).

In an interesting study, Basso and coworkers analyzed the chemical nature of the surfaces of two enzymes, lipase B from *Candida antarctica* (CALB) and penicillin G acylase from *Providence rettgeri* (PGA), and its influence on the immobilization process on various supports.[6] In particular, the distribution of the regions of the protein able to establish either hydrophobic or hydrophilic interactions was studied by means of the GRID computational method, which calculates the molecular fields generated by the interaction of a chemical probe (water or an aliphatic carbon) with the enzyme surface.[6] **Figure 3** (top) shows that in CALB, whose catalytic function is exerted at the lipid/water interface, the hydrophilic zones (blue areas) are clearly differentiated from the hydrophobic ones (yellow areas). In particular, a broad hydrophilic region is opposite to the active site, which implies that the orientation of CALB can be modulated varying the hydrophilicity of the carrier.[6] In contrast, the PGA surface (**Figure 3**, bottom) exhibits a homogeneous distribution of both hydrophilic and hydrophobic regions.

4. Mesoporous silica as protein binders

Zeolites, which comprise one of the most important families of porous materials, present small pore size (below 1.2 nm) that somehow limits their application for immobilization of proteins.[51] In contrast, amorphous mesoporous silicas have several advantages such as uniform and higher pore diameters (2-40 nm), surface areas in the range 300-1500 $m^2 g^{-1}$ and high pore volumes (*ca* 1 $ml\ g^{-1}$). Recently, ordered mesoporous silicas (**Figure 4**) have emerged as potentially ideal carriers because, in addition the aforementioned features, they present a good connectivity of the porous networks and it is possible to select the textural properties including the pore shape (channel-like or cage-like). Several enzymes have been successfully immobilized in

ordered mesoporous silicas; in particular, Serra *et al.* adsorbed the lipase CALB, whose dimensions are approx. 3 x 4 x 5 nm, in the cage-like material SBA-16, synthesized with the surfactant Pluronic F128.[52] The lixiviation of the enzyme was practically eliminated, which suggests that a compromise between diffusional restrictions and enzyme leaching must be encountered for optimal performance of the immobilized biocatalyst. Besides, the hydrophilic-lipophilic balance (HLB) of the silica can be easily modulated by chemical modification with alkyltriethoxysilane and it was demonstrated to exert an influence on enzyme loading, catalytic activity and lixiviation.[19,53]

Several one-step processes for the simultaneous synthesis of ordered porous silica networks by sol-gel technique and enzyme encapsulation within the pores have been described.[54,55] The enzyme molecules are entrapped in isolated silica cages connected by small entrances (bottle-around-the-ship), thus allowing the diffusion of substrates and products but avoiding enzyme leakage. Various amphiphiles such as cationic surfactants (cetyltrimethylammonium bromide, CTAB) or Pluronic triblock copolymers have been tested as silica structure directors. Compared with the post-synthesis adsorption strategy, simultaneous synthesis/encapsulation leads to well structured materials with higher enzyme loading.

5. Analysis of the distribution of the enzyme in the support

Fluorescence confocal microscopy, which renders spatial information about the distribution of fluorescent compounds over the radius of a bead,[56] is being successfully employed to visualize the distribution of biomolecules throughout the support as well as to evaluate restrictions to diffusion within the support.[57] A typical confocal image for sterol esterase[58] labeled with fluorescein isothiocyanate (FTIC) and covalently immobilized in epoxy-activated Dilbeads™ TA is shown in **Figure 5**, varying the

observation depth.[22] Interestingly, the enzyme was not uniformly distributed in the beads, as most of the enzyme molecules were confined in an outer shell of approximately 10.5 μm width. The depth of the enzyme layer was very similar analyzing beads of different radius. Thus, there is an apparent restriction for diffusional transport into the core of the bead, which can be caused, among other factors, by the tortuosity of the pore structure, or by the steric hindrance exerted by the enzyme molecules that are immobilized in the shell of the particle. Similar conclusions were reported for the immobilization of trypsin on porous glycidyl methacrylate beads,[56] whereas a uniform enzyme distribution throughout the bed was observed for glucose oxidase in alginate microspheres, obtained by *in situ* enzyme entrapment.[57]

6. Conclusions

The topic of enzyme immobilization continues to attract great interest in the industry sector because it requires stable and robust immobilized enzymes to withstand necessary harsh conditions of operation. The lack of guidelines that could govern the selection of the immobilization method is being replaced by a rational design of immobilized derivatives, in which the protein 3D structure (and reactivity) as well as the textural properties of the support are important parameters. An important feature is that the carrier not only functions as a scaffold for the protein molecules but also alters the enzyme properties. *In silico* analyses may help to establish the optimal immobilization conditions and to understand the behaviour of immobilized enzymes.

One of the major challenges currently facing material scientists is the development of tailor-made carriers with specific physical and chemical properties, e.g. suitable geometry and binding properties, which can be used in different reactor configurations and bionanodevices. Novel concepts such as the application of ordered

mesoporous (organo)silicas as enzyme adsorbents or the entrapment of enzymes in a spatially restricted sol-gel matrix promise exciting research and advances in the next few years. In addition, the combination of different immobilization techniques, which provide high enzyme loading and high retention of activity, will increasingly be used.

ACKNOWLEDGEMENTS

Project BIO2010-20508-C04-01 from Spanish Ministry of Science and Innovation supported this research. P. T-S and B. R-C were supported by fellowships from Comunidad de Madrid and Spanish Ministry of Science and Innovation (FPI program), respectively.

Reference List

1. M. Alcalde, M. Ferrer, F.J. Plou, A. Ballesteros, *Trends Biotechnol.* **2006**, *24*, 281.
2. R.A. Sheldon, *Adv. Synth. Catal.* **2007**, *349*, 1289.
3. M. Ferrer, F.J. Plou, G. Fuentes, M.A. Cruces, L. Andersen, O. Kirk, M. Christensen, A. Ballesteros, *Biocatal. Biotransform.* **2002**, *20*, 63.
4. J. Ge, D. Lu, Z. Liu, Z. Liu, *Biochem. Eng. J.* **2009**, *44*, 53.
5. L. Cao, *Curr. Opin. Chem. Biol.* **2005**, *9*, 217.
6. A. Basso, P. Braiuca, S. Cantone, C. Ebert, P. Linda, P. Spizzo, P. Caimi, U. Hanefeld, G. Degrassi, L. Gardossi, *Adv. Synth. Catal.* **2007**, *349*, 877.
7. P. Braiuca, C. Ebert, A. Basso, P. Linda, L. Gardossi, *Trends Biotechnol.* **2006**, *24*, 419.
8. S. Hudson, E. Magner, J. Cooney, B. Kieran, *J. Phys. Chem. B* **2005**, *109*, 19496.
9. E. Weber, D. Sirim, T. Schreiber, B. Thomas, J. Pleiss, M. Hunger, R. Gläser, V.B. Urlacher, *J. Mol. Catal. B-Enzym.* **2010**, *64*, 29.
10. D.F.M. Neri, V.M. Balcao, F.O.Q. Dourado, J.M.B. Oliveira, J. Carvalho, J.A. Teixeira, *J. Mol. Catal. B-Enzym.* **2011**, *70*, 74.
11. B. Sahoo, S.K. Sahu, P. Pramanik, *J. Mol. Catal. B-Enzym.* **2011**, *69*, 95.
12. M. Azodi, C. Falamaki, A. Mohsenifar, *J. Mol. Catal. B-Enzym.* **2011**, *69*, 154.
13. R. Reshmi, G. Sanjay, S. Sugunan, *Catal. Commun.* **2006**, *7*, 460.
14. R. Reshmi, G. Sanjay, S. Sugunan, *Catal. Commun.* **2007**, *8*, 393.
15. W. Limbut, P. Thavarungkul, P. Kanatharana, P. Asawatreratanakul, C. Limsakul, B. Wongkittisuksa, *Biosens. Bioelectron.* **2004**, *19*, 813.
16. D.F.M. Neri, V.M. Balcao, F.O.Q. Dourado, J.M.B. Oliveira, J. Carvalho, J.A. Teixeira, *J. Mol. Catal. B-Enzym* **2011**, *70*, 74.
17. Y. Ren, J.G. Rivera, L. He, H. Kulkarni, D.K. Lee, P.B. Messersmith PB, *BMC Biotechnol*, DOI: 10.1186/1472-6750-11-63.
18. F.N. Serralha, J.M. Lopes, M.R. Aires-Barros, D.M.F. Prazeres, J.M.S. Cabral, F. Lemos, F. Ramoa Ribeiro, *Enzyme Microb. Tech.* **2002**, *31*, 29.
19. Y. Xu, G. Zhou, C. Wu, T. Li, H. Song, *Solid State Sci.* **2011**, *13*, 867.
20. A. Kumar, S.S. Kanwar, *Bioresource Technol.* **2011**, *102*, 2162.
21. I. Ghazi, A. Gomez de Segura, L. Fernandez-Arrojo, M. Alcalde, M. Yates, M.L. Rojas-Cervantes, F.J. Plou, A. Ballesteros, *J. Mol. Catal. B-Enzym.* **2005**, *35*, 19.

22. P. Torres, A. Datla, V.W. Rajasekar, S. Zambre, T. Ashar, M. Yates, M.L. Rojas-Cervantes, O. Calero-Rueda, V. Barba, M.J. Martinez, A. Ballesteros, F.J. Plou, *Catal. Commun.* **2007**, *9*, 539.

23. H.A. Akdogan, N.K. Pazarlioglu, *Process Biochem.* **2011**, *46*, 840.

24. H. Kawakita, K. Sugita, K. Saito, M. Tamada, T. Sugo, H. Kawamoto, *J. Membrane Sci.* **2002**, *205*, 175.

25. P. Torres, D. Reyes-Duarte, N. Lopez-Cortes, M. Ferrer, A. Ballesteros, F.J. Plou, *Process Biochem.* **2008**, *43*, 145.

26. I. Roy, S. Sharma, M.N. Gupta, *Adv. Biochem. Eng. Biotechnol.* **2004**, *86*, 159.

27. D. Kubac, A. Cejkova, J. Masak, V. Jirku, M. Lemaire, E. Gallienne, J. Bolte, R. Stloukal, L. Martinkova, *J. Mol. Catal. B-Enzym.* **2006**, *39*, 59.

28. A.C. Pierre, *Biocatal. Biotransform.* **2004**, *22*, 145.

29. M. Filho, B.C. Pessela, C. Mateo, A.V. Carrascosa, R. Fernandez-Lafuente, J.M. Guisan, *Process Biochem.* **2008**, *43*, 1142.

30. H.V. Adikane, R.K. Singh, D.M. Thakar, S.N. Nene, *Appl. Biochem. Biotech.* **2001**, *94*, 127.

31. A. Manrich, A. Komesu, W.S. Adriano, P.W. Tardioli, R.L.C. Giordano, *Appl. Biochem. Biotech.* **2010**, *161*, 455.

32. T. Boller, C. Meier, S. Menzler, *Org. Process Res. Dev.* **2002**, *6*, 509.

33. K. Buchholz, V. Kasche, U.T. Bornscheuer, in *Biocatalysts and Enzyme Technology*, Wiley-VCH, Weinheim, Germany **2005**.

34. J. Torres-Bacete, M. Arroyo, R. Torres-Guzman, I. de la Mata, M.P. Castillon, C. Acebal, *J. Chem. Technol. Biotechnol.* **2001**, *76*, 525.

35. C. Mateo, R. Torres, G. Fernandez-Lorente, C. Ortiz, M. Fuentes, A. Hidalgo, F. Lopez-Gallego, O. Abian, J.M. Palomo, L. Betancor, B.C.C. Pessela, J.M. Guisan, R. Fernandez-Lafuente, *Biomacromolecules* **2003**, *4*, 772.

36. P. Wang, S. Dai, S.D. Waezsada, A.Y. Tsao, B.H. Davison, *Biotechnol. Bioeng.* **2001**, *74*, 249.

37. M.T. Martin, M. Alcalde, F.J. Plou, A. Ballesteros, *Indian J. Biochem. Biophys.* **2002**, *39*, 229.

38. A. Gomez de Segura, M. Alcalde, M. Yates, M.L. Rojas-Cervantes, N. Lopez-Cortes, A. Ballesteros, F.J. Plou, *Biotechnol. Prog.* **2004**, *20*, 1414.

39. E. Katchalski-Katzir, D.M. Kraemer, *J. Mol. Catal. B-Enzym.* **2000**, *10*, 157.

40. L. Cao, *Carrier-bound immobilized enzymes: Principles, applications and design*, Wiley-VCH, Weinheim, Germany **2005**.

41. Y. Zhang, J.L. Xu, D. Li, Z.H. Yuan, *Biocatal. Biotransform.* **2010**, *28*, 313.

42. P.J. Halling, R.V. Ulijn, S.L. Flitsch, *Curr. Opin. Biotech.* **2005**, *16*, 385.

43. A. del Monte-Martinez, B. Cutiño-Avila, in *Methods in Molecular Biology, Lipases and Phospholipases: Methods and Application*, (Eds: G. Sandoval.), Humana Press, Totowa, NJ, USA **2011**, Ch. 20

44. A. Kunamneni, I. Ghazi, S. Camarero, A. Ballesteros, F.J. Plou, M. Alcalde, *Process Biochem.* **2008**, *43*, 169.

45. H. Li, A.D. Robertson, J.H. Jensen, *Proteins* **2005**, *61*, 704.

46. W. Hartmeier, *Trends Biotechnol.* **1985**, *3*, 149.

47. E. Severac, O. Galy, F. Turon, C.A. Pantel, J.S. Condoret, P. Monsan, A. Marty, *Enzyme Microb. Tech.* **2011**, *48*, 61.

48. S.K. Karmee, *Appl. Microbiol. Biot.* **2009**, *81*, 1013.

49. P. Torres, A. Poveda, J. Jimenez-Barbero, A. Ballesteros, F.J. Plou, *J. Agric. Food Chem.* **2010**, *58*, 807.

50. J.A. Bosley, J.C. Clayton, *Biotechnol. Bioeng.* **1994**, *43*, 934.

51. A. Macario, A. Katovic, G. Giordano, L. Forni, F. Carloni, A. Filippini, L. Setti, *Stud. Surf. Sci. Catal.* **2005**, *155*, 381.

52. E. Serra, A. Mayoral, Y. Sakamoto, R.M. Blanco, I. Diaz, *Micropor. Mesopor. Mat.* **2008**, *114*, 201.

53. E. Serra, E. Diez, I. Diaz, R.M. Blanco, *Micropor. Mesopor. Mat.* **2010**, *132*, 487.

54. A. Macario, M. Moliner, A. Corma, G. Giordano, *Micropor. Mesopor. Mat.* **2009**, *118*, 334.

55. S. Urrego, E. Serra, V. Alfredsson, R.M. Blanco, I. Diaz, *Micropor. Mesopor. Mat.* **2010**, *129*, 173.

56. M. Malmsten, K.Z. Xing, A. Ljunglof, *J. Colloid Interf. Sci.* **1999**, *220*, 436.

57. H. Zhu, R. Srivastava, Q. Brown, M.J. McShane, *Bioconjugate Chem.* **2005**, *16*, 1451.

58. O. Calero-Rueda, V. Barba, E. Rodriguez, F. Plou, A. Martinez, M.J. Martinez, *BBA-Protein. Proteom.* **2009**, *1794*, 1099

Table 1. Materials used as carriers for enzyme immobilization and the binding methodologies.

Type of material	Examples	Immobilization method	Reference
Inorganic supports			
Alumina, Zirconia	Aminoalkylsilane-alumine	Adsorption, Covalent	[13,14]
Silica	Controlled-pore glass (CPG), Hexadecyl silica	Adsorption, Covalent	[15]
Iron oxides	Coated magnetic nanoparticles	Adsorption, Covalent	[16,17]
Zeolites	Na Y Zeolite	Adsorption	[18]
Mesoporous silica	SBA-15, FDU-12	Adsorption, Covalent, Encapsulation	[19]
Diatomaceous soil	Celite	Adsorption	[20]
Organic polymers			
Polyacrylamide	Eupergit C	Covalent	[21]
Polymethacrylate	Sepabeads, Dilbeads	Covalent	[22]
Poly(styrene-codivinylbenzene)	Amberlite XAD-7	Adsorption	[23]
	Dowex SBR-P, Amberlite IRC50, Duolite A-7	Ionic adsorption	[24]
Polypropylene	Accurel EP-100	Adsorption	[25]
Smart polymers	Poly-N-isopropylacrylamide	Covalent	[26]
Hydrogels			
Polyvinyl alcohol	Lentikats	Entrapment	[27]
Silica sol-gel	Xerogels, Aerogels	Entrapment	[28]
Biopolymers			
Modified polysaccharides	DEAE-Cellulose[a], DEAE-Dextran[a], CM-Agarose[b]	Ionic adsorption	[29]
	Octyl-Agarose, Cellulose esters	Hydrophobic adsorption	[30]
	Glyoxyl-Agarose, CNBr-activated Sepharose[c]	Covalent	[31]

[a] DEAE: Diethylaminoethyl; [b] CM: Carboxymethyl; [c] CNBr: Cyanogen bromide

Table 2. Reactivity calculations through *LIGRe* algorithm for the *M. thermophila* laccase at pH 9.0.

Ionizable Group	**pK_a (PROPKA)**	***LIGRe* (pH 9)**
N-Term	8.0	10.0
Tyr^{286}	9.12	0.75
Tyr^{214}	9.66	0.21
Lys^{128}	9.80	0.15
Tyr^{391}	9.83	0.14
Lys^{339}	9.94	0.11
Lys^{56}	10.08	0.08
Tyr^{546}	10.21	0.06
Lys^{205}	10.22	0.06
Lys^{353}	10.22	0.06
Lys^{454}	10.22	0.06
Lys^{374}	10.29	0.05
Lys^{325}	10.29	0.05
Tyr^{305}	10.33	0.05
Lys^{119}	10.36	0.04

Table 3. RDID predictions for the *M. thermophila* laccase immobilization in various support materials.

Support	S_{BET} [$m^2\ g^{-1}$]	***mMQ*** [$\mu mol\ g^{-1}$]	***tMQ*** [$mg\ g^{-1}$]
Polyamide (Accurel PA-6)	7.4	0.35	24.5
Polypropylene (Accurel EP-100)	78.9	3.68	260.9
Amberlite IRA-900	240	11.2	793.5
Glyoxyl-Sepharose CL 2B	11.4	0.52	37.8
Glyoxyl-Sepharose CL 4B	23.6	1.10	77.9
Glyoxyl-Sepharose CL 6B	35.7	1.67	118.1
Sepabeads EC-EP3	43.0	2.01	142.6
Eupergit C	57.0	2.66	188.4
Eupergit C 250 L	49.3	2.30	163.0

Figure legends

Fig. 1. Protocols for covalent immobilization of enzymes: (a) binding to epoxy-activated carriers through amino or phenolic groups; (b) activation of amino supports with glutaraldehyde and further binding with amino groups of the enzyme or with mannoses of glycoproteins; (c) activation of hydroxyl moieties of supports with cyanogen bromide and coupling to amino enzyme groups.

Fig. 2. Surface model of the 3D structure of *M. thermophila* laccase showing all reactive groups at pH 9.0: a) Left view; b) Front view; c) Right view; d) Rotation of 35° of the 3D structure (left view) visualizing the active site; e) Amplification of the region close to the active site showing the surface reactive residues that could affect the catalytic activity. (**----**) Position of the NH_2-terminal.

Fig. 3. Comparison of the molecular interaction fields generated by interaction of lipase from *Candida antarctica* B (top pictures) and penicillin G acylase (bottom pictures) with an aliphatic carbon probe (yellow, on the left) and with the water probe (blue, on the right) calculated by the GRID program. With permission from Reference [6].

Fig. 4. Structure of several ordered mesoporous silica. Starting from the left: SBA-15 (*p6mm*), KIT-6 (*Ia-3d*), SBA-16 (*Im-3m*) and FDU-12 (*Fm-3m*). From Reference [52].

Fig. 5. Confocal images of FITC-labelled crude sterol esterase immobilized on Dilbeads TA. The images were obtained by taking different deep z-section scans with 5 μm depth increment between each picture from A to D. With permission from Reference [22].

Fig. 1.

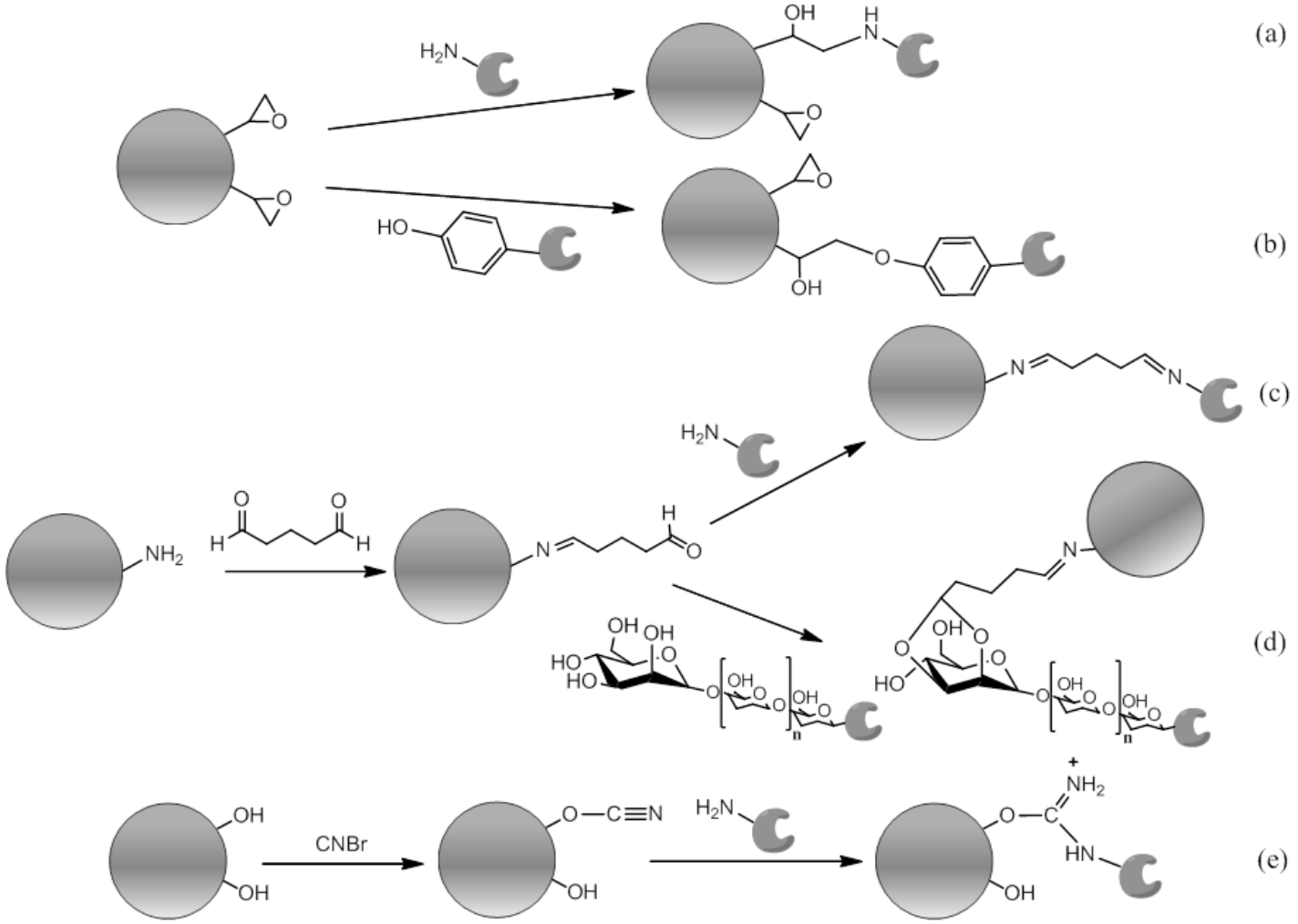

Fig. 2

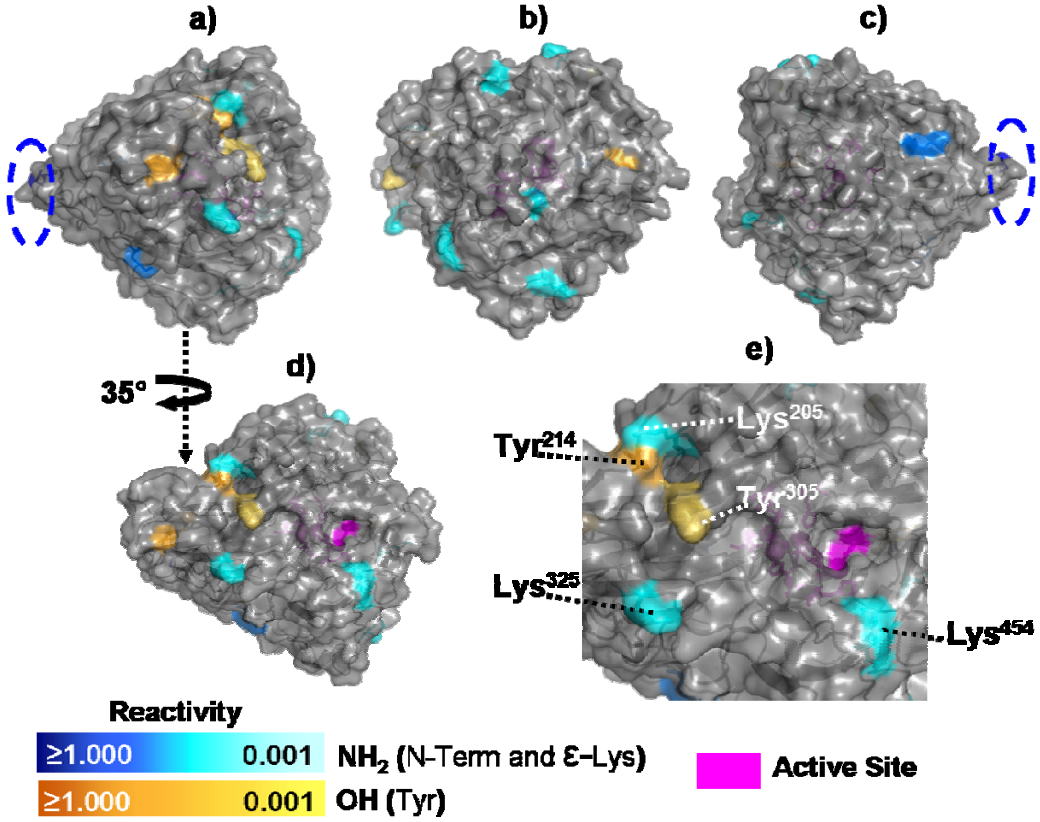
a)
b)
c)
d)
e)
35°
Lys205
Tyr214
Tyr305
Lys325
Lys454
Reactivity
≥1.000
0.001
NH2 (N-Term and ε-Lys)
≥1.000
0.001
OH (Tyr)
Active Site

Fig. 3

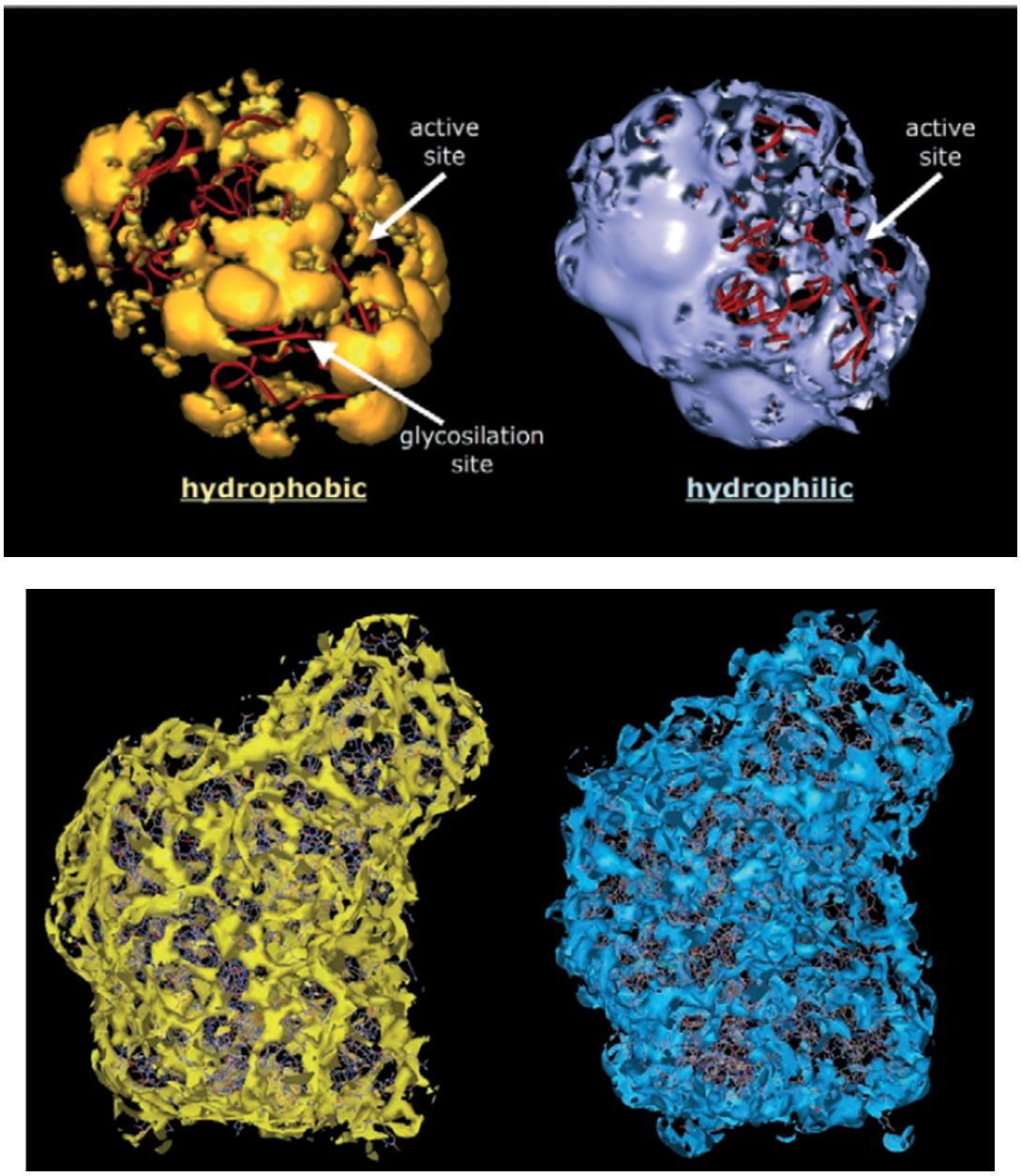
active site
glycosilation site
hydrophobic
active site
hydrophilic

Fig. 4

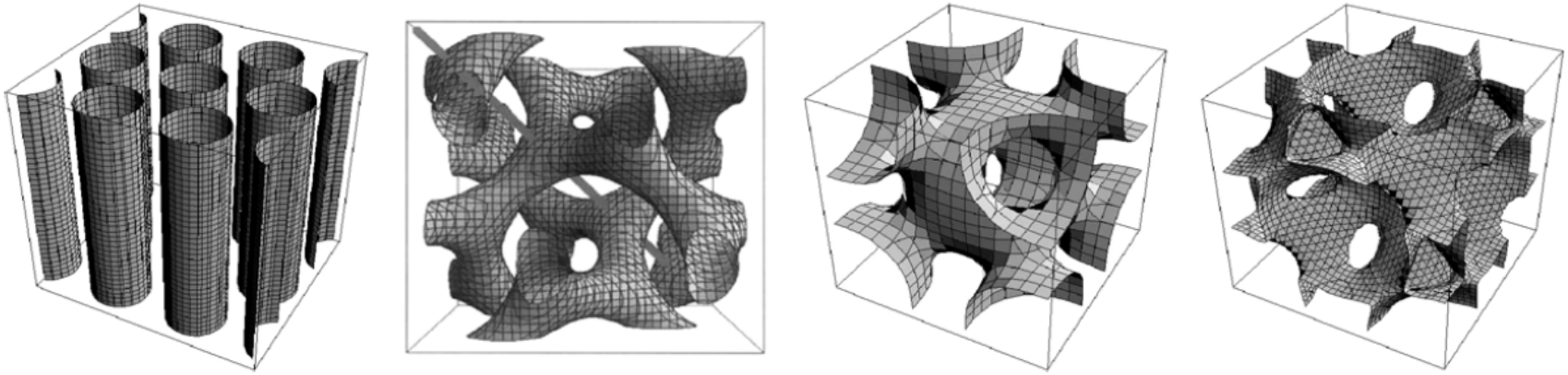

Fig. 5